Study of mechanical and dielectric spectrum in YFe$_{1-x}$Mn$_x$O$_3$ ceramics

Weili Zhu, Ju He, Yaming Jin, Ruixia Ti, Tingting Xu, Chen Yue, Fengzhen Huang, Xiaomei Lu, Feng Yan, and Jinsong Zhu

View Online   Export Citation   CrossMark

ARTICLES YOU MAY BE INTERESTED IN

The multiferroic perovskite YFeO$_3$
Applied Physics Letters **102**, 062903 (2013); https://doi.org/10.1063/1.4791697

Relaxorlike dielectric behavior and weak ferromagnetism in YFeO$_3$ ceramics
Journal of Applied Physics **103**, 124111 (2008); https://doi.org/10.1063/1.2947601

Magnetocapacitance effect in nonmultiferroic YFeO$_3$ single crystal
Journal of Applied Physics **111**, 034103 (2012); https://doi.org/10.1063/1.3681294

Study of mechanical and dielectric spectrum in YFe$_{1-x}$Mn$_x$O$_3$ ceramics

Weili Zhu,[1] Ju He,[1] Yaming Jin,[1] Ruixia Ti,[1] Tingting Xu,[1] Chen Yue,[1] Fengzhen Huang,[1] Xiaomei Lu,[1,a)] Feng Yan,[2,b)] and Jinsong Zhu[1,c)]

[1]*National Laboratory of Solid State Microstructures and Physics School, Nanjing University, Nanjing 210093, China*
[2]*Department of Applied Physics, Hong Kong Polytechnic University, Hong Kong, China*

The mechanical spectra of Mn-substituted yttrium orthoferrite YFe$_{1-x}$Mn$_x$O$_3$ (x = 0, 0.2, 0.3, 0.4) ceramics were performed at kilohertz from 100 to 360 K. Two internal friction (IF) peaks are observed around 150 K and 230 K, respectively, and both the IF peaks exhibit frequency dispersion behavior. The IF peak around 150 K is associated with a step increase in the modulus and its mechanical relaxation rate follows the Vogel-Fulcher relation with $\tau_0 = 4.45 \times 10^{-11}$s, $E_\alpha = 0.03$ eV, and $T_{VF} = 155$ K. This IF peak can be explained in terms of a freezing of oxygen vacancies after excluding the possible magnetic spin glass transition. Another IF peak around 230 K presents a relaxation behavior and it follows Arrhenius law. Furthermore, the relaxation behavior was verified by the dielectric spectrum and it can be ascribed to the charge carrier hopping between Fe^{2+} and Fe^{3+}. © *2014 AIP Publishing LLC.*
[http://dx.doi.org/10.1063/1.4862301]

I. INTRODUCTION

The doping and substituting with different types of magnetic ions are usually a very useful experimental technique to understand, modify, and enhance the properties of the compound. Multiferroic materials have drawn an increasing amount of interest due to their potential applications in many multi-functional devices.[1–3] As a typical rare-earth orthoferrite, YFeO$_3$ indicates the antiferromagnetic nature with a high Néel temperature (T$_N$ = 640 K) and a high resistivity.[4,5] The weak ferromagnetic behavior is generally produced in YFeO$_3$ by an antisymmetric exchange interaction.[6] Although the normal ferroelectricity is not expected in YFeO$_3$ according to its centrosymmetric space group Pnma, the electronic ferroelectricity may exist.[7] YMnO$_3$ is one of the single-phase multiferroic materials and it belongs to the space group of P6$_3$cm with a high ferroelectric transition temperature (T$_C$ ∼ 900 K) and a low antiferromagnetic transition temperature (T$_N$ ∼ 70 K).[8–11] The ferroelectricity of YMnO$_3$ is the result of distortion of the layered MnO$_5$ polyhedra, accompanied by a displacement of the Y ions and there is a coupling between the ferroelectric and antiferromagnetic order in YMnO$_3$.[8,9] Recent studies have demonstrated the occurrence of the magnetodielectric effect and the ferroelectricity at different temperature scales in Mn-substituted yttrium orthoferrite ceramics and their dielectric characteristics, ferroelectric and magnetic properties have also been investigated.[12,13] Mechanical spectrum is a well-known probe for the study of phase transitions and relaxations of micro-units, such as point defects, dislocations, grain boundaries, and domain walls in solids.[14–25] Up to now, few works have reported about mechanical spectra

study of YFeO$_3$ and Mn-doped YFeO$_3$ ceramics.[26,27] In this paper, the study on the internal friction (IF) and dielectric properties of YFe$_{1-x}$Mn$_x$O$_3$ (x = 0, 0.2, 0.3, 0.4) ceramics is presented. Two internal friction peaks are observed for the samples of all composition. One may be relative with the emergence of freezing of the oxygen vacancies and the other one is attributed to the dipolar effects induced by charge carrier hopping motions for the emergency of Fe^{2+}, the latter was further verified by the dielectric spectrum.

II. EXPERIMENTS

YFe$_{1-x}$Mn$_x$O$_3$ ceramics (with x = 0, 0.2, 0.3, 0.4) were prepared by the citrate sol-gel route. Primarily, stoichiometric amounts of Y(NO$_3$)$_3$·6H$_2$O (99.99%), Mn(CH$_3$COO)$_2$·4H$_2$O (99.0%), and Fe(NO$_3$)$_3$·9H$_2$O(98.5%) were dissolved in de-ionized water with the total metal ions concentration around 0.2M. The resulting solution was held for 4 h under constant stirring. Citric acid (C$_6$H$_8$O$_7$) in 1:1 molar ratio with respect to the total metal ions was added to the solution as a complexant and the mixtures were stirred until transparent. Then the transparent system was heated in oil bath at 150 °C to obtain dry powders. The obtained precursor powders were ground and heated at 300 °C for 3 h in air. All of the powders were calcined at 900 °C for 6 h in air which enable the formation of the desired oxides. The resulting powders were reground again and pressed into rectangular bars. The bars were sintered at 1350 °C for 12 h in air. Pt electrodes were sputtered on the pellets and bars for electrical and internal friction measurements, respectively.

The crystal structures of the samples were analyzed by powder X-ray diffraction using Cu $K\alpha$ radiation. The combination states of Fe2p and Mn2p electrons were examined by X-ray photoelectron spectroscopy (XPS, Thermo ESCALAB). Dielectric properties were characterized by a HP4194A impedance analyzer. The mechanical spectra were measured for

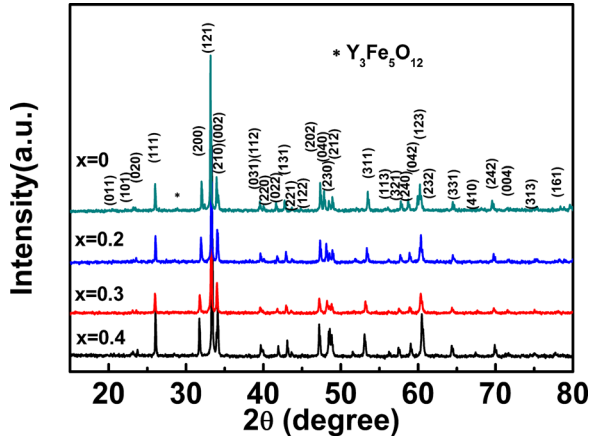a)xiaomeil@nju.edu.cn
b)apafyan@polyu.edu.cn
c)jszhu@nju.edu.cn

FIG. 1. Room temperature powder x-ray diffraction patterns of $YFe_{1-x}Mn_xO_3$ (x = 0, 0.2, 0.3, 0.4) samples.

rectangular bars ($40 \times 4 \times 0.3$ mm^3) in the free-free flexural vibration mode from 100 to 360 K at the resonance frequency about several kilohertz. A combination of electrostatic drive and capacitor microphone detection (PJ-II type Video Frequency Internal Friction Device) was used with the details described in Ref. 20. The two-node mode (about kHz) and three-node mode (about 2.8 times kHz) were used to change the measuring frequency, respectively. The experiments were conducted on cooling at a rate of about 2.0 k/min and on heating at about 1.0 k/min. A Dynamic Mechanical Analyzer (Perkin-Elmer DMA 8000) was used to measure the IF in Hz frequency.

III. RESULTS AND DISCUSSION

Figure 1 shows the room temperature powder x-ray diffraction patterns of $YFe_{1-x}Mn_xO_3$ (x = 0, 0.2, 0.3, 0.4) ceramics. All samples with different compositions show single orthorhombic phase the same as $YFeO_3$ in space group Pnma(62) without other impurity phase. With increasing amount of Mn, some peaks tend to merge together, which indicates the appearance of lattice distortion after substituting Mn for Fe. This is in agreement with previous results by Cao *et al.*[28] The lattice distortion may cause the displacement of ions and then lead to the normal ferroelectricity like $YMnO_3$.
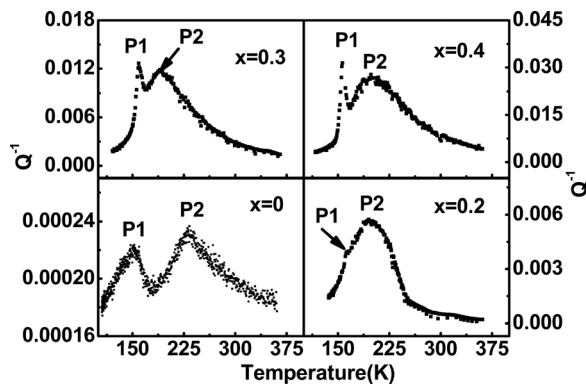

FIG. 2. Temperature dependence of internal friction of $YFe_{1-x}Mn_xO_3$ (x = 0, 0.2, 0.3 and 0.4) ceramics.

Figure 2 depicts the internal friction spectra of $YFe_{1-x}Mn_xO_3$ with x = 0, 0.2, 0.3, and 0.4 at 100–360 K on the heating process. Two internal friction peaks are observed for all samples. They locate around 150 K and 230 K (labeled as P1 and P2) in undoped $YFeO_3$ sample. With the substitution of Mn for Fe, the peak position of the P1 peak is almost no change, while the P2 peak shifts toward lower temperature in the samples. And the IF peak height also shows an increase with increasing of x in $YFe_{1-x}Mn_xO_3$ (x = 0.2, 0.3, 0.4) samples.

Figure 3 represents the temperature-dependent reduced Young's modulus ($\frac{\Delta Y}{Y_0} = \frac{Y-Y_0}{Y_0} \propto \frac{f^2-f_0^2}{f_0^2}$), the f and f_0 are the

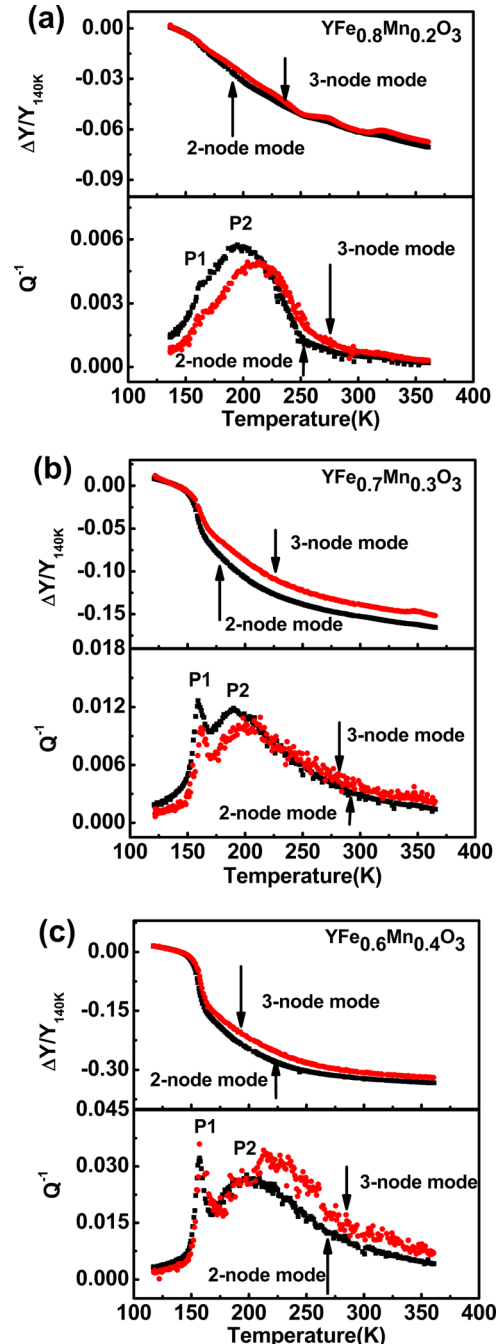FIG. 3. Temperature dependence of reduced Young's modulus $\frac{\Delta Y}{Y_{140K}} = \frac{Y-Y_{140K}}{Y_{140K}}$ and internal friction Q^{-1} in the heating process for $YFe_{0.8}Mn_{0.2}O_3$ (a), $YFe_{0.7}Mn_{0.3}O_3$ (b), and $YFe_{0.6}Mn_{0.4}O_3$ (c).

resonance frequency and the one at a fixed temperature, respectively. The internal friction Q^{-1} measured about 1900 Hz (two-node mode) and about 5300 Hz (three-node mode) is shown in Figures 3(a) ($YFe_{0.8}Mn_{0.2}O_3$), 3(b) ($YFe_{0.7}Mn_{0.3}O_3$), and 3(c) ($YFe_{0.6}Mn_{0.4}O_3$) samples on heating. The P1 peak accompanies with a small step increase in the reduced modulus for $YFe_{0.8}Mn_{0.2}O_3$ sample and the step increase shows more obvious in $YFe_{0.7}Mn_{0.3}O_3$ and $YFe_{0.6}Mn_{0.4}O_3$ samples. In the temperature-dependent IF in Figure 3, P1 peak shows a slight dependence on the measuring frequency. The shifts of peak temperature only 1.6 k, 1.89 K, and 1.78 K of P1 peak, which shows an intrinsic feature of the frequency dependence and it is not due to the experimental errors. For P1 peak, the relaxation time τ is satisfied with the following equation:

$$\omega\tau = 1, \quad (1)$$

where $\omega = 2\pi f$ is the resonance circle frequency. Usually, relaxation time is assumed to follow an Arrhenius law

$$\tau = \tau_0 \exp(E_\alpha/k_B T), \quad (2)$$

where E_α is the activation energy, τ_0 the relaxation time constant, and k_B Boltzmann constant. The activation energy can be calculated from the shift of peak temperature with the variation of the resonance frequency

$$\frac{E_\alpha}{k_B} = \frac{\ln(f_2/f_1)}{1/T_1 - 1/T_2}, \quad (3)$$

where f_1 and T_1, f_2 and T_2 are the resonance frequency and peak temperature about 1900 Hz and 5300 Hz. The very large activation energy 1.4 eV, 1.16 eV, and 1.17 eV and unreasonable small relaxation time constants $\tau_{01} = 3.40 \times 10^{-50}$ s, $\tau_{02} = 2.04 \times 10^{-41}$ s, $\tau_{03} = 1.07 \times 10^{-42}$ s are obtained for $YFe_{0.8}Mn_{0.2}O_3$, $YFe_{0.7}Mn_{0.3}O_3$, and $YFe_{0.6}Mn_{0.4}O_3$ samples, respectively. Based on above discussion, the Arrhenius law can be safely excluded for P1 peak. Another possible relaxation, the Vogel-Fulcher (VF) relation (glassy freezing) may match this relaxation behavior. However, two measuring frequencies only (about 1900 and 5300 Hz) can be used for the limitation of our instrument. The limited range of frequencies accessible makes it difficult to compare Vogel-Fulcher (glassy freezing) model for the response. To clarify the mechanism of this P1, the low-frequency internal friction and modulus at Hz frequency range were measured by a DMA using a single cantilever bending mode at a heating rate of 2 K/min. Figure 4(a) shows the temperature dependence of internal friction and modulus for the $YFe_{0.6}Mn_{0.4}O_3$ sample at 0.1, 0.2, 0.5, 1, 2 Hz, respectively. Figure 4(b) is the temperature dependence of the relaxation rate (hollow circles: the experimental data; solid circles: fitting to the VF relation)[29]

$$\tau = \tau_0 \exp\{E_\alpha/[k_B \cdot (T - T_{VF})]\}, \quad (4)$$

where T_{VF} is the Vogel-Fulcher temperature. A good straight line with the following parameters $\tau_0 = 4.45 \times 10^{-11}$ s, $E_\alpha = 0.03$ eV, and $T_{VF} = 155$ K was obtained. The VF
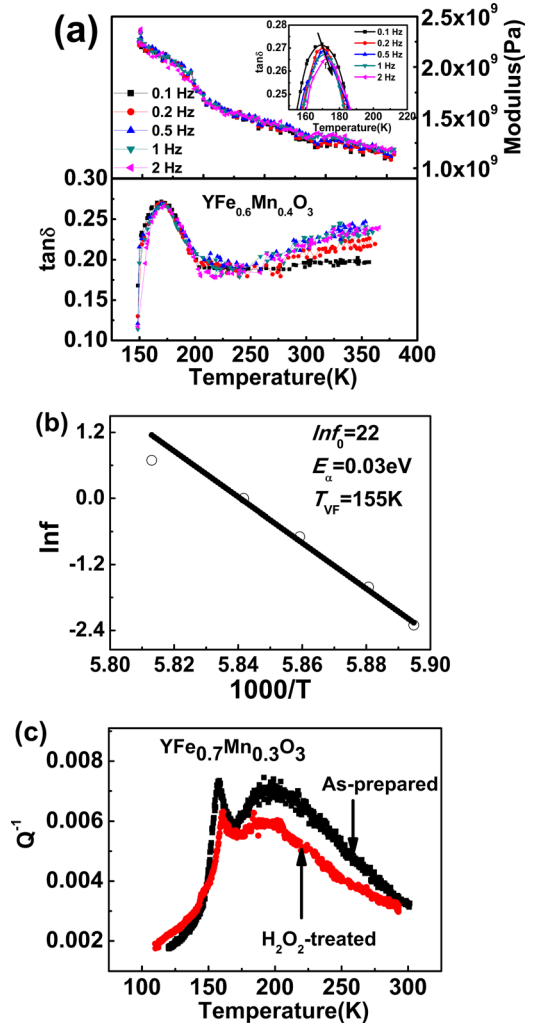

FIG. 4. (a) Temperature dependence of low-frequency internal friction and modulus for the $YFe_{0.6}Mn_{0.4}O_3$ sample with various frequencies. The upper-right inset shows $\tan\delta$ on expanded scales at low temperature. (b) Temperature dependence of the relaxation rate (hollow circles: the experimental data; solid circles: fitting to the Vogel-Fulcher relation). (c) Temperature dependence of internal friction Q^{-1} for as-prepared and H_2O_2-treated $YFe_{0.7}Mn_{0.3}O_3$ ceramic on heating route.

relation appears usually in the glassy transition process. Two possible origins may match this relaxation in our samples: one is the magnetic spin glass behavior, the spin "frozen," which just like our previous work in $Ho_3Fe_5O_{12}$[30] and another is the defects, such as the oxygen vacancies freezing process.[31]

About the magnetic related transitions in YFMO system,[12,32] the one is the paramagnetic to antimagnetic transition at the Néel point T_N (above 300 K) and upon the substitution of Mn for Fe, a spin-reorientation transition is observed at T_{SR}, where the antiferromagnetic easy axis initially oriented along the a axis changes its direction to the b axis. However, the T_{SR} increases with increasing Mn content and it is not the case for peak temperature of P1 and P2. The peak temperature of P1 is almost no change with Mn content and the P2 peak temperature is decreasing with Mn content. Otherwise, no split was observed in our magnetic measurements (M-T curves) under field cooling (FC) and zero field cooling (ZFC), which implies no spin glassy transition here. Therefore, both our two IF peaks do not relate with the

magnetic transitions. Usually, oxygen vacancies exist in the perovskite oxides[33] and an IF peak fitted the Vogel-Fulcher relation in $YBa_2Cu_3O_{7-\delta}$ superconductor around 220 K was observed and it was suggested to be the freezing of oxygen vacancies in Ref. [31]. The P1 peak may also be ascribed to the freezing transition, glassy behaviors of the oxygen vacancies. In order to confirm the oxygen vacancies freezing transition-related origin for the P1 peak, a treatment in different oxygen atmosphere for $YFe_{0.8}Mn_{0.2}O_3$, $YFe_{0.7}Mn_{0.3}O_3$ and $YFe_{0.6}Mn_{0.4}O_3$ samples was carried out. Figure 4(c) shows the temperature-dependent reduced Young's modulus and internal friction measured about 1900 Hz for as-prepared and oxygen-treated $YFe_{0.7}Mn_{0.3}O_3$ sample only. The intensity of P1 peak is strongly depressed after oxygen treatment, which implies the oxygen vacancies dependence of P1 peak. The P1 peak is relative with the freezing of the oxygen vacancies.

The P2 peak is observed around 230 K as shown in Figures 3(a)–3(c) for three samples with different Mn content. It is a broad peak and shifts to higher temperature with increasing measuring frequencies, which indicates that the peak is associated with thermally activated processes[34] and it is further verified by the dielectric spectrum. Figures 5(a)–5(c) depict the temperature dependence of imaginary components M'' of the dielectric modulus for x = 0.2, x = 0.3, and x = 0.4 samples in the frequency range from $10^{2.5}$ Hz to 10^6 Hz.[35] A dielectric relaxation behavior is observed in temperature range of 150–330 K for the samples with different compositions. The activation energy (E_α) for this relaxation can be fitted by the famous Arrhenius law. The well fitted lines are obtained in the upper-right insets of Figures 5(a)–5(c). The values of activation energy E_α calculated from the slope of the fitting straight line are 0.32 eV, 0.30 eV, and 0.28 eV for the three compositions. They are very close to the activation energy of a two-site polaron hopping process of charge transfer between transition metal ions under different valence states.[36–38] To make certain which transition metal ion the dielectric relaxation behavior originates from, the combination states of Fe2p and Mn2p electron were examined by XPS technique. The XPS results confirm that Fe ions are present in Fe^{2+} and Fe^{3+} states and Mn ions are present in Mn^{3+} state mainly (XPS scan of the $Mn2p_{3/2}$ lines are not shown here). The upper-left insets of Figures 5(a)–5(c) show representative XPS scan of the Fe $2p_{3/2}$ lines for $YFe_{0.8}Mn_{0.2}O_3$, $YFe_{0.7}Mn_{0.3}O_3$, and $YFe_{0.6}Mn_{0.4}O_3$ samples, respectively. The binding energy of $Fe2p_{3/2}$ was reported to appear at 709.3 eV for Fe^{2+} and at 710.7 eV for Fe^{3+}.[39] Using the Lorentzian-Gaussian curve fitting method, the mixed peak can be fitted by two peaks, corresponding to Fe^{2+} and Fe^{3+} states. The estimated ratio of $Fe^{2+}:Fe^{3+}$ is 5:33, 5:26, and 5:19 for x = 0.2, x = 0.3, x = 0.4, respectively, and the trivalent state is dominant in all the three compositions. The coexistence of Fe^{2+} and Fe^{3+} is reasonable for oxygen loss during sample preparation and Fe^{2+} is generated subsequently for charge compensation.[40,41] The P2 peak comes from the charge transfer between Fe^{2+} and Fe^{3+}. Additionally, the intensity of P2 peak is strengthened and the activated energy decreases with increasing Mn content for the ratio of $Fe^{2+}:Fe^{3+}$ changing from 5:33 to
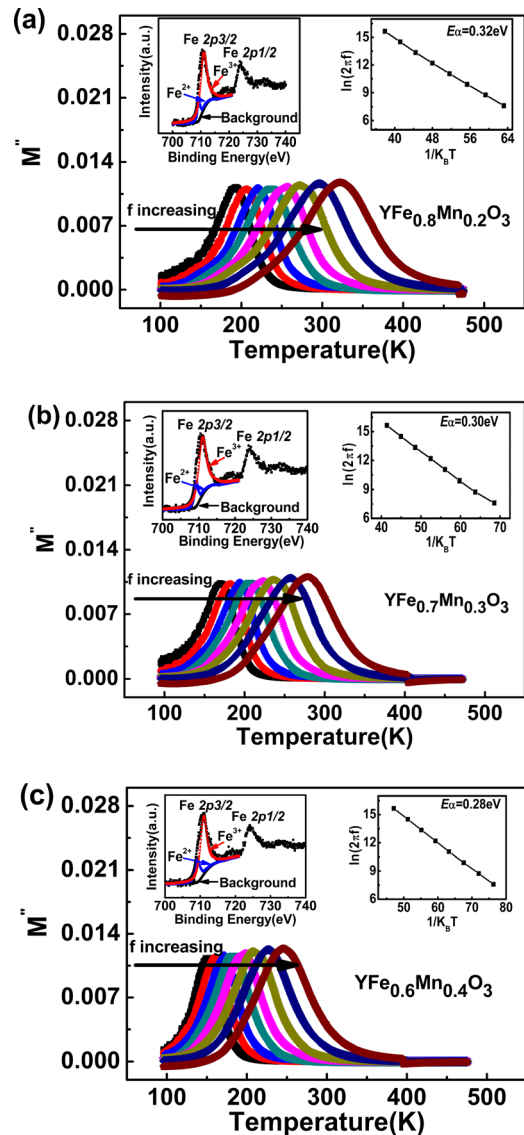

FIG. 5. Temperature dependence of the imaginary components of the dielectric modulus M'' for $YFe_{0.8}Mn_{0.2}O_3$ (a), $YFe_{0.7}Mn_{0.3}O_3$ (b), and $YFe_{0.6}Mn_{0.4}O_3$ (c) measured at various frequencies of $10^{2.5}$, 10^3, $10^{3.5}$, 10^4, $10^{4.5}$, 10^5, $10^{5.5}$, and 10^6 Hz. The upper-left and the lower-right insets of (a), (b), and (c) depict the Arrhenius fitting (solid line) for the peak temperature of M'' and the Lorentzian-Gaussian dividing of the Fe $2p_{3/2}$ core level, respectively.

5:19. More two-site electron hopping processes appear with increasing in Fe^{2+} content rate as increasing of Mn doping. The decrease in activation energy for electron hopping between Fe^{2+} and Fe^{3+} may indicate that the hopping is a collective behavior instead of an individual one.[42] The correlation for the hopping electrons increases with an increase in the concentration of Fe^{2+} ions and the activation energy thus decreases.

IV. CONCLUSIONS

The mechanical spectra (IF and modulus) of $YFe_{1-x}Mn_xO_3$ (x = 0, 0.2, 0.3, 0.4) ceramics were performed by kilohertz and Hz frequencies. Two IF peaks around 150 k and 230 K are observed and both of them are frequency dispersion. The former can be fitted with the VF relation and it

can be explained in terms of a possible freezing of oxygen vacancies. The latter relaxation behavior obeys the Arrhenius law and it can be ascribed to the charge carrier hopping between Fe^{2+} and Fe^{3+}. The relaxation behavior was further verified by the dielectric spectrum.

ACKNOWLEDGMENTS

[1] W. Eerenstein, N. D. Mathur, and J. F. Scott, Nature (London) **442**, 759 (2006).

[2] G. Catalan, Appl. Phys. Lett. **88**, 102902 (2006).

[3] J. Hemberger, P. Lunkenheimer, R. Fichtl, H.-A. Krug von Nidda, V. Tsurkan, and A. Loidl, Nature (London) **434**, 364 (2005).

[4] T. M. Rearick, G. L. Catchen, and J. M. Adams, Phys. Rev. B **48**, 224 (1993).

[5] M. Eibschütz, S. Shtrikman, and D. Treves, Phys. Rev. **156**, 562 (1967).

[6] S. Mathur, M. Veith, R. Rapalaviciute, H. Shen, G. F. Goya, W. L. W. Filho, and T. S. Berquo, Chem. Mater. **16**, 1906 (2004).

[7] N. Ikeda, H. Ohsumi, K. Ohwada, K. Ishii, T. Inami, K. Kakurai, Y. Murakami, K. Yoshii, S. Mori, Y. Horibe, and H. Kito, Nature (London) **436**, 1136 (2005).

[8] B. B. Van Aken, T. T. M. Palstra, A. Filippetti, and N. A. Spaldin, Nature Mater. **3**, 164 (2004).

[9] Z. J. Huang, Y. Cao, Y. Y. Sun, Y. Y. Xue, and C. W. Chu, Phys. Rev. B **56**, 2623 (1997).

[10] C. Moure, J. F. Fernandez, M. Villegas, and P. Duran, J. Eur. Ceram. Soc. **19**, 131 (1999).

[11] G. Lescano, F. M. Figueiredo, F. M. B. Marques, and J. Schmidt, J. Eur. Ceram. Soc. **21**, 2037 (2001).

[12] P. Mandal, V. S. Bhadram, Y. Sundarayya, C. Narayana, A. Sundaresan, and C. N. R. Rao, Phys. Rev. Lett. **107**, 137202 (2011).

[13] Y. Ma, Y. J. Wu, Y. Q. Lin, and X. M. Chen, J. Mater. Sci.: Mater. Electron. **21**, 838 (2010).

[14] A. S. Nowick and B. S. Berry, *Anelastic Relaxation in Crystalline Solid* (Academic Press, New York, 1972).

[15] R. K. Zheng, R. X. Huang, A. N. Tang, G. Li, X. G. Li, J. N. Wei, J. P. Shui, and Z. Yao, Appl. Phys. Lett. **81**, 3834 (2002).

[16] Y. H. Yuan, X. N. Ying, and L. Zhang, J. Appl. Phys. **110**, 053515 (2011).

[17] C. Wang, S. A. T. Redfern, M. Daraktchiev, and R. J. Harrison, Appl. Phys. Lett. **89**, 152906 (2006).

[18] X. S. Wu, H. L. Zhang, J. R. Su, C. S. Chen, and W. Liu, Phys. Rev. B **76**, 094106 (2007).

[19] X. N. Ying and Z. C. Xu, J. Appl. Phys. **105**, 063504 (2009).

[20] Y. H. Yuan and X. N. Ying, Solid State Sci. **14**, 84 (2012).

[21] H. Kong and C. Zhu, Appl. Phys. Lett. **88**, 041920 (2006).

[22] H. Kong and C. Zhu, J. Phys.: Condens. Matter **20**, 115211 (2008).

[23] F. Cordero, F. Trequattrini, V. B. Barbeta, R. F. Jardim, and M. S. Torikachvili, Phys. Rev. B **84**, 125127 (2011).

[24] X. N. Ying, Z. C. Xu, and X. M. Wang, Solid State Commun. **148**, 91 (2008).

[25] X. N. Ying and L. Zhang, Solid State Commun. **152**, 1252 (2012).

[26] A. K. Zvezdin and A. A. Mukhin, Z. Eksp. Teor. Fiz. **102**, 577 (1992).

[27] J. Krzywinski, J. Magn. Magn. Mater. **59**, 62 (1986).

[28] X. Q. Cao, C.-S. Kim, and H.-I. Yoo, J. Am. Ceram. Soc. **84**, 1265 (2001).

[29] H. Vogel, Z. Phys. **22**, 645 (1921); G. Fulcher, J. Am. Ceram. Soc. **8**, 339 (1925).

[30] J. Su, X. M. Lu, C. Zhang, J. T. Zhang, H. Sun, C. C. Ju, Z. J. Wang, K. l. Min, F. Z. Huang, and J. S. Zhu, Physica B **407**, 485 (2012).

[31] T. Lægreid and K. Fossheim, Europhys. Lett. **6**, 81 (1988).

[32] P. Mandal, C. R. Serrao, E. Suard, V. Caignaert, B. Raveau, A. Sundaresan, and C. N. R. Rao, J. Solid State Chem. **197**, 408 (2013).

[33] F. Cordero, A. Franco, V. R. Calderone, P. Nanni, and V. Buscaglia, J. Eur. Ceram. Soc. **26**, 2923 (2006).

[34] W. J. Lu, B. C. Zhao, R. Ang, W. H. Song, J. J. Du, and Y. P. Sun, Phys. Lett. A **346**, 321 (2005).

[35] P. L. Meena, R. Kumar, C. L. Prajapat, K. Sreenivas, and V. Gupta, J. Appl. Phys. **106**, 024105 (2009).

[36] Y. Kohara, Y. Yamasaki, Y. Onose, and Y. Tokura, Phys. Rev. B **82**, 104419 (2010).

[37] Y. Yamasaki, Y. Kohara, and Y. Tokura, Phys. Rev. B **80**, 140412 (2009).

[38] Y. J. Wu, Y. Gao, and X. M. Chen, Appl. Phys. Lett. **91**, 092912 (2007).

[39] F. Z. Huang, X. M. Lu, W. W. Lin, X. M. Wu, Y. Kan, and J. S. Zhu, Appl. Phys. Lett. **89**, 242914 (2006).

[40] Y. Ma, X. M. Chen, and Y. Q. Lin, J. Appl. Phys. **103**, 124111 (2008).

[41] J. Su, X. M. Lu, C. Zhang, J. T. Zhang, S. Peng, X. B. Wu, K. L. Min, F. Z. Huang, and J. S. Zhu, J. Mater. Sci. **46**, 3488–3492 (2011).

[42] J. Su, X. M. Lu, J. T. Zhang, H. Sun, C. Zhang, Z. H. Jiang, C. C. Ju, Z. J. Wang, F. Z. Huang, and J. S. Zhu, J. Appl. Phys. **111**, 014112 (2012).